CHEMISTRY
A EUROPEAN JOURNAL

DOI: 10.1002/chem.201102816

Dinucleosides with Non-Natural Backbones: A New Class of Ribonuclease A and Angiogenin Inhibitors

Joy Debnath,[b] Swagata Dasgupta,*[a] and Tanmaya Pathak*[a]

Abstract: Ribonuclease A (RNase A) serves as a convenient model enzyme in the identification and development of inhibitors of proteins that are members of the ribonuclease superfamily. This is principally because the biological activity of these proteins, such as angiogenin, is linked to their catalytic ribonucleolytic activity. In an attempt to inhibit the biological activity of angiogenin, which involves new blood vessel formation, we employed different dinucleosides with varied non-natural backbones. These compounds were synthesized by coupling aminonucleosides with dicarboxylic acids and amino- and carboxynucleosides with an amino acid. These molecules show competitive inhibition with inhibition constant (K_i) values of (59 ± 3) and (155 ± 5) μM for RNase A. The compounds were also found to inhibit angiogenin in a competitive fashion with corresponding K_i values in the micromolar range. The presence of an additional polar group attached to the backbone of dinucleosides was found to be responsible for the tight binding with both proteins. The specificity of different ribonucleolytic subsites were found to be altered because of the incorporation of a non-natural backbone in between the two nucleosidic moieties. In spite of the replacement of the phosphate group by non-natural linkers, these molecules were found to selectively interact with the ribonucleolytic site residues of angiogenin, whereas the cell binding site and nuclear translocation site residues remain unperturbed. Docked conformations of the synthesized compounds with RNase A and angiogenin suggest a binding preference for the thymine–adenine pair over the thymine–thymine pair.

Keywords: angiogenin · cell binding site · inhibitors · nucleosides · ribonuclease A

Introduction

Several members of the ribonuclease (RNase) superfamily display a multitude of activities in addition to the catalytic activity normally associated with these proteins. Angiogenin is one such member that is a potent inducer of angiogenesis, the process of new blood vessel formation.[1,2] The processes of tumor growth, invasion, and metastasis are dependent upon angiogenesis and angiogenin is known to induce many steps of this complex cascade.[3–8] Tumors and cancer cells are known to use this process for ready access to nutrients.[9] The biological activity of angiogenin is dependent on its ribonucleolytic activity.[10] Eosinophil-derived neurotoxin (EDN) is a catalytically efficient RNase with its ribonucleolytic activity being essential for its neurotoxic, helminthotoxic, and antiviral activities.[11] RNase activity is also required for the antiviral and neurotoxic activity of eosinophil cationic protein (ECP).[12] Thus the design of inhibitors of the catalytic activity of ribonucleolytic proteins is expected to have an indirect effect on their purported biological activity. The homology of these proteins with ribonuclease A (RNase A) permits its use as a model system in the development of inhibitors.

The catalytic site of RNase A contains various different subsites. Hydrolysis of the phosphodiester bond occurs at the P_1 subsite that is composed of His-12, Lys-41, and His-119 residues. Similarly, His-13, Lys-40, and His-114 residues constitute the P_1 subsite of angiogenin (Figure 1), which bears about 65% identity with RNase A. Apart from the P_1 subsite, these two proteins have two other important subsites for the recognition of nucleobases of their substrate (RNA), namely B_1 and B_2 subsites. A comparison of the ribonucleolytic sites of these two proteins is given in Figure 1. The B_1 and B_2 subsites are known for their pyrimidine and purine specificity, respectively.[13] The ribonucleolytic activity of angiogenin, though 10^{-5}–10^{-6} weaker[14,15] than RNase A, is nevertheless essential for its biological activity.[16,17] The designed low-molecular-weight inhibitors for the biologically active RNases have been tested on bovine pancreatic RNase A as a model protein of this superfamily.

Reports of many nucleotidic inhibitors for RNase A with very low K_i values do exist.[18,19] These nucleotidic inhibitors have limited success for angiogenin. Despite the fact that

[a] Prof. S. Dasgupta, Prof. T. Pathak
Department of Chemistry
Indian Institute of Technology Kharagpur
Kharagpur-721302 (India)
Fax: (+91) 3222-255303
E-mail: swagata@chem.iitkgp.ernet.in
tpathak@chem.iitkgp.ernet.in

[b] Dr. J. Debnath
Department of Pharmaceutical Sciences
University of Tennessee
847 Monroe, Johnson Bldg, Room 331
Memphis, Tennessee 38163 (USA)

Supporting information for this article is available on the WWW under http://dx.doi.org/10.1002/chem.201102816.

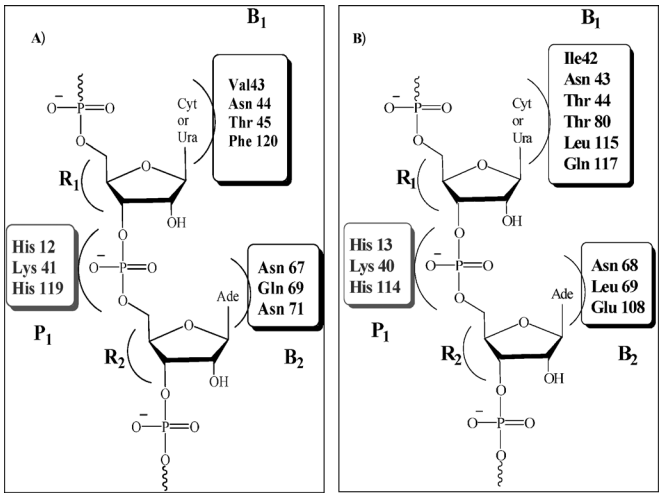

Figure 1. Key residues of ribonucleolytic site (A) RNase A and (B) angiogenin.

these molecules completely mimic the substrate of RNases and bind strongly with these enzymes, there appear to be two basic problems regarding their administration in the body. First, there is the difficulty associated with the transport of these compounds through the biological membrane. The high negative charge on the phosphate group makes them difficult to use in vivo.[20–24] Second, the possible hydrolysis of the polyphosphate group by different enzymes present in body fluid namely Ap_3A hydrolase, Ap_4A hydrolase and diphosphoinositol polyphosphate phosphohydrolases (DIPP proteins) are likely to render them ineffective. Apart from these features, their possible toxicity and likely accumulation of degraded products in the body, which can inhibit essential system pathways, cannot be overlooked.[21]

Our attempt to develop nucleoside-based inhibitors with carboxylic and amino functionalities showed successful inhibition of the ribonucleolytic activity of RNase A.[25–27] In this study, a non-natural backbone was used to link two nucleosidic moieties in lieu of the phosphate or pyrophosphate groups.[18–24] This linkage minimizes the ionic character of the compounds. Two sets of backbone-modified dinucleosides have been designed, one with a nonpolar backbone and the other set of compounds with a polar backbone. The amide bond was selected to connect the modified nucleosidic units, because of their expected stability towards phosphohydrolases. The nature of the linkers between the nucleosidic moieties has also been varied by altering the spacer length and polar groups. The variant nature of the linkers is expected to produce valuable information about their mode of binding with the proteins.

Results and Discussion

The basic skeleton chosen for the dinucleoside inhibitors developed in this study are based on thymidine and adenosine. Two sets of backbone-modified dinucleosides, one with a nonpolar backbone and the other set of compounds with polar backbones have been synthesized. In order to prepare these backbone-modified dinucleosides, the nonparticipating functional groups of nucleosides were masked with appropriate protecting groups. The protecting groups were selected in a manner such that the number of deprotection steps was minimized for regenerating the functional groups of nucleosides.

For the synthesis of these dinucleosides, two monomeric nucleosidic moieties were prepared individually, one with carboxylic and the other with an amino group. To generate the thymidine monomeric unit with one carboxylic group we started with compound **1**.[25] Thus, the amino group of partially protected aminothymidine **1** was treated with succinic and glutaric anhydride to produce compounds **2** and **3**, respectively (Scheme 1).

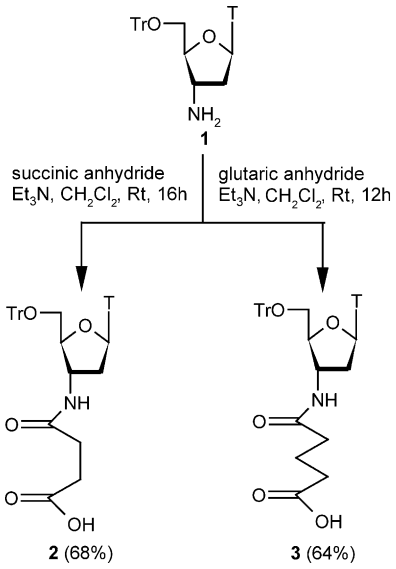

Scheme 1. Synthesis of aminonucleoside-dicarboxylic acid hybrids **2** and **3**.

5′-Carboxy thymidine **6** was prepared from partially protected thymidine **4**[28] by oxidation of the 5′-OH group using $K_2S_2O_8$ as the oxidizing agent and $RuCl_3$ as a catalyst (Scheme 2).[29] Compound **5**, with an amino group at the 5′-position, was obtained from thymidine using a reported method.[30] 2′,3′-Protected 5′-carboxyadenosine **9** was synthesized from partially protected adenosine **7** (Scheme 3) and

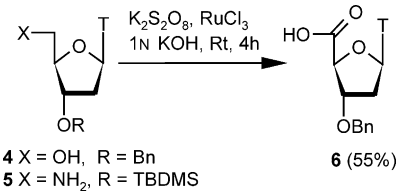

Scheme 2. Synthesis of 5′-carboxythymidine **6** from compound **4**.

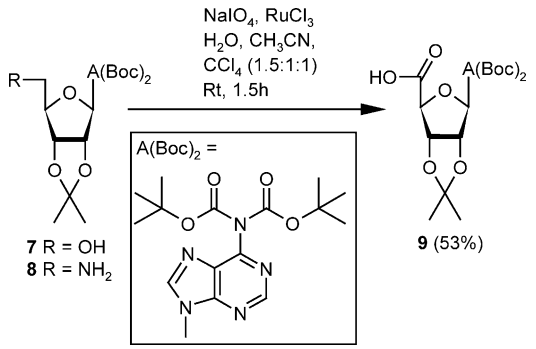

Scheme 3. Synthesis of 5′-carboxyadenosine analogue **9** from compound **7**.

the 5′-amino-5′-deoxyadenosine derivative **8** was prepared from adenosine using a literature procedure.[31]

The thymidine monomeric units **2** and **3** were coupled separately with **5** through amide bonds to produce modified dinucleosides with nonpolar backbones (Scheme 4) by using

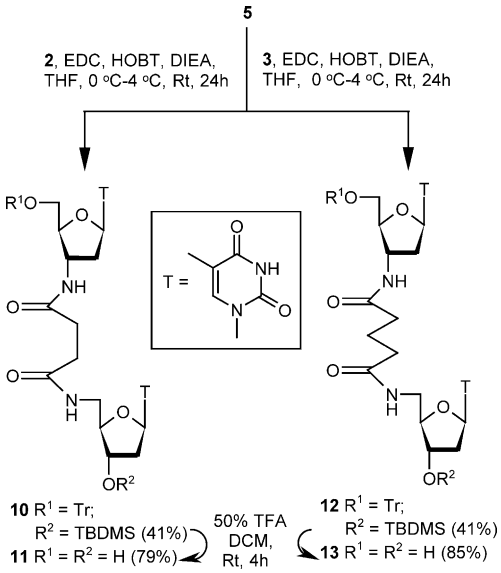

Scheme 4. Synthesis of dinucleosides **11** and **13** with neutral backbones.

a combination of 1-[3-(dimethylamino)propyl]-3-ethylcarbodiimide (EDC) and 1-hydroxybenzotriazole (HOBT) as coupling reagent and diisopropylethylamine (DIEA) as the base to obtain fully protected dimers **10** and **12**, respectively.[32] Since compound **12** was always contaminated with an inseparable impurity the compound was directly taken to the deprotection step. All acid-labile groups of **10** and **12** were removed in one step by 50% TFA treatment to afford the required dimeric nucleosides **11** and **13**, respectively (Scheme 4). A similar strategy was used for the synthesis of a dinucleoside **15**, in which thymidine and adenosine analogues were linked with a nonpolar backbone. Thus aminonucleoside/succinic acid hybrid **2** was coupled with the adenosine analogue **8** to obtain the fully protected dimer **14**. All acid-labile trityl, isopropylidene and *tert*-butoxycarbonyl masking groups were removed in one step with the help of 50% TFA treatment to afford the heterodimer **15** (Scheme 5).

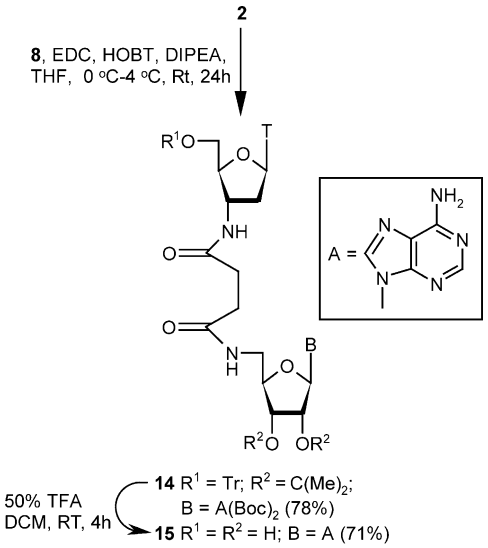

Scheme 5. Synthesis of heterodimer **15** with neutral backbone.

For the introduction of a carboxylic group in the internucleoside bond of a dinucleoside, a partially protected aspartic acid derivative L-Boc-Asp(OBzl)OH was selected. To reduce the number of deprotection steps, a benzyl group was selected for the protection of γ-carboxylic group of aspartic acid and 3′/5′-group of thymidine. Although in general it was difficult to synthesize a 5′-*O*-benzyl-protected aminonucleoside from the corresponding azidonucleoside keeping the benzyl group intact, the use of $SnCl_2$-PhSH-Et_3N[33] led to the reduction of azidothymidine **16**[34] to give the benzyl-protected aminothymidine **17** in moderate yield (Scheme 6). Compound **17** was coupled with L-Boc-Asp(OBzl)OH using dicyclohexylcarbodiimide (DCC) and *N*-hydroxysuccinamide (NHS) to afford fully protected nucleoside amino acid conjugate **18**. Selective deprotection of the Boc group of **18** with a mixture of 4 M TMSCl and 4 M PhOH afforded compound **19** with one free amino group (Scheme 6). Modified dinucleosides with polar backbones were then prepared by separately coupling **19** with carboxynucleosides **6** and **9** to afford fully protected dinucleosides **20** and **22**, respectively. In case of **20** all the three benzyl groups were removed by using Pd/C under H_2 atmosphere to afford the homodinucleoside **21**. For the synthesis of the heterodimer **23**, the benzyl groups of **22** were removed by using the same procedure mentioned above and the remaining Boc and the isopropylidene groups were removed by 50% TFA in dichloromethane (Scheme 6).

The inhibition of the ribonucleolytic activity of RNase A was checked by agarose-gel-based assay, for which the degradation of tRNA by RNase A was monitored (Figure 2). The most intense band observed in lane 1 was due to the

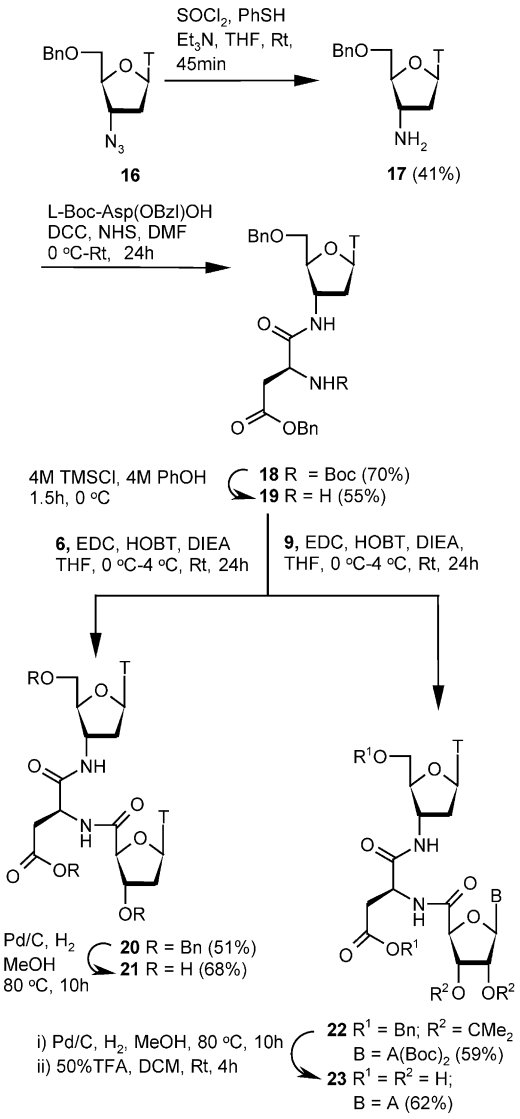

Scheme 6. Synthesis of homodimer **21** and heterodimer **23** with polar backbone.

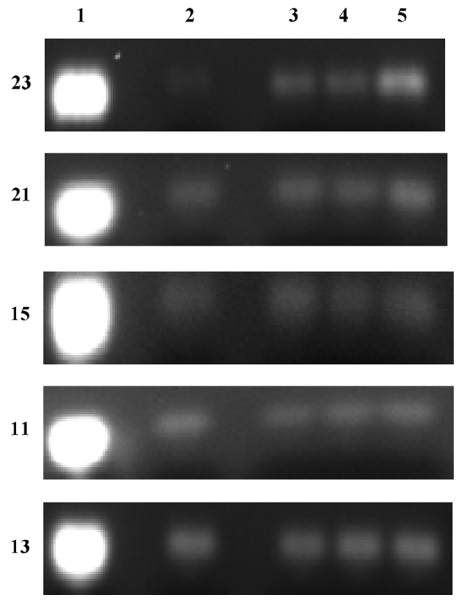

Figure 2. Agarose-gel-based assay. RNase concentration: 0.5 μM and concentration of all compounds 0.92 mM. Lane1: tRNA; Lane 2: tRNA and RNase A; Lanes 3, 4 and 5: tRNA and RNase A with increasing concentration of inhibitors.

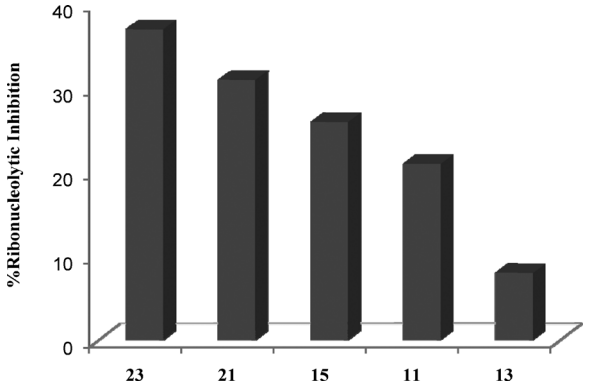

Figure 3. Ribonucleolytic inhibition of RNase A by backbone modified dinucleosides (**23**, **21**, **15**, **11**, and **13**). RNase A and compound concentration are 0.27 μM and 0.7 mM respectively.

presence of the control, tRNA. The maximum possible degradation of tRNA by RNase A resulted in the faint intensity of the band observed in lane 2. The differential intensity of bands in lanes 3 to 5 indicate the extent of RNase A inhibition by the compounds at three different concentrations (lower to higher concentrations, respectively). These results qualitatively showed a better inhibition potency of **15**, **21**, and **23** compared to the other compounds.

The histogram of relative ribonucleolytic activities obtained from the precipitation assay at a particular inhibitor concentration (0.7 mM) further confirmed the comparative inhibitory efficacy of the backbone modified nucleosides (Figure 3). It was observed that compounds with a carboxylic functionality between two nucleoside moieties (**21** and **23**) showed better inhibition. It was also observed that the thymine–adenine pair showed better inhibitory potential over the thymine–thymine pair. This was probably because of the better anchoring of the thymine–adenine base pair at B_1 and B_2 sites respectively.

To determine the nature of inhibition and the inhibition constants, kinetic experiments were conducted with **23**, **21**, **15**, and **11**. The inhibition constant values (K_i) obtained for **23**, **21, 15**, and **11** were (59 ± 3), (155 ± 5), (443 ± 2) and (544 ± 2) μM, respectively. From the nature of the Dixon plots of the four compounds (Figure 4 A–D) it was confirmed that the mode of inhibition was competitive in nature. The order of values obtained for the inhibition constants correlated well with the previous agarose gel and precipitation assay.

After the kinetic experiments, we proceeded with docking studies to visualize the conformation of the synthesized

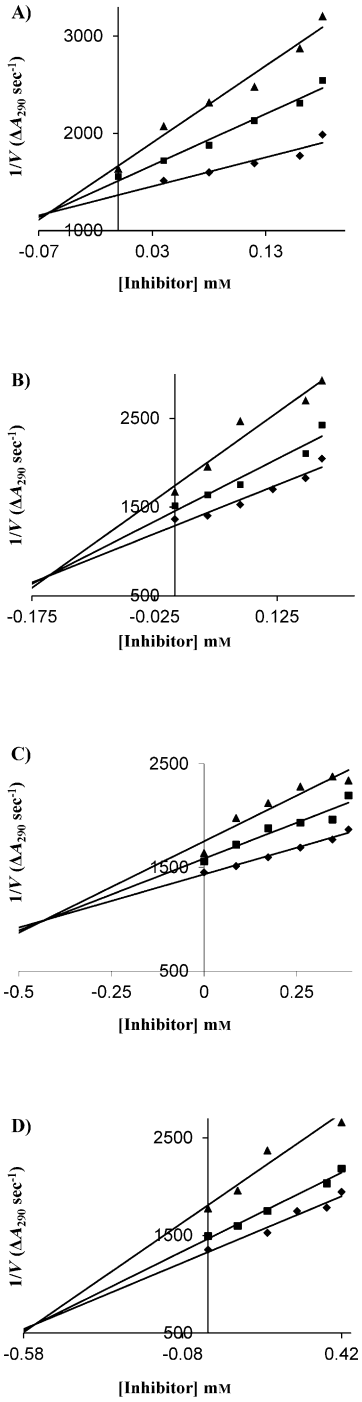

Figure 4. Dixon plots for RNase A inhibition by A) Compound **23**: substrate concentrations: 580 μM (◆), 320 μM (■) and 275 μM (▲); B) Compound **21**: substrate concentrations: 650 μM (◆), 490 μM (■) and 320 μM (▲); and C) Compound **15**: substrate concentrations: 500 μM (◆), 350 μM (■) and 220 μM (▲). D) Compound **11**: substrate concentrations: 750 μM (◆), 500 μM (■) and 350 μM (▲). The RNase A concentration: 7.5 μM.

compounds in the protein. From the docked conformation of compound **23**, we found that its carboxylic group was within hydrogen-bonding distance of both His-12 and Lys-41. On the other hand the 2′- and 3′-OH groups of adenosine were in a position to form a five-membered ring with the $N^{\delta 1}$ atom of His-119 by means of a possible hydrogen-bonding network (Figure 5A). It was found that in spite of the presence of the thymine nucleobase the carboxylic moiety occupied the B_1 site of the protein.

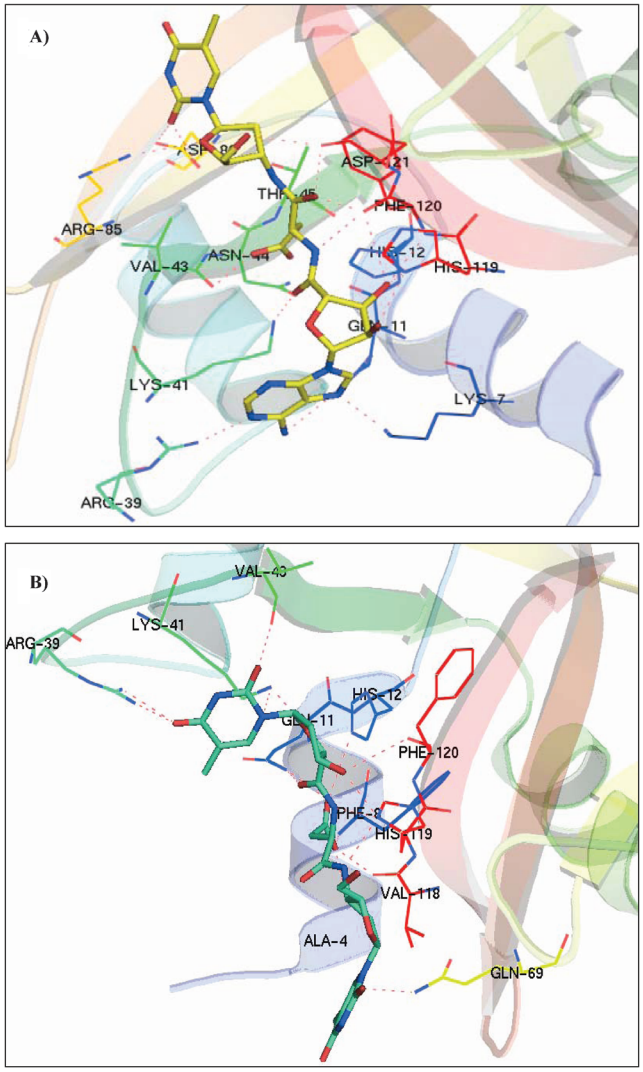

Figure 5. Docked conformation of A) **23** (yellowish-green) and B) **21** (green) with RNase A (1FS3).

The docked conformation of **21** also showed the same mode of interaction, but in this case one of the thymine moieties interacted with the B_1 site (Val-43) residue (Figure 5B). The carboxylic group of this compound interacted only with the His-12 residue, whereas for **23** the carboxylic group interacted with both His-12 and Lys-41. For molecule **21**, it was observed that the nitrogen atoms of the linker amide bond were in a position to form a five-membered ring through a hydrogen-bonding network with the $N^{\delta 1}$ atom of His-119 similar to **23**.

In the docked conformation of compound **15**, it was found that the adenine moiety was in close proximity to His-119, His-12, and Lys-41 (Figure 6A). Here we also find that the

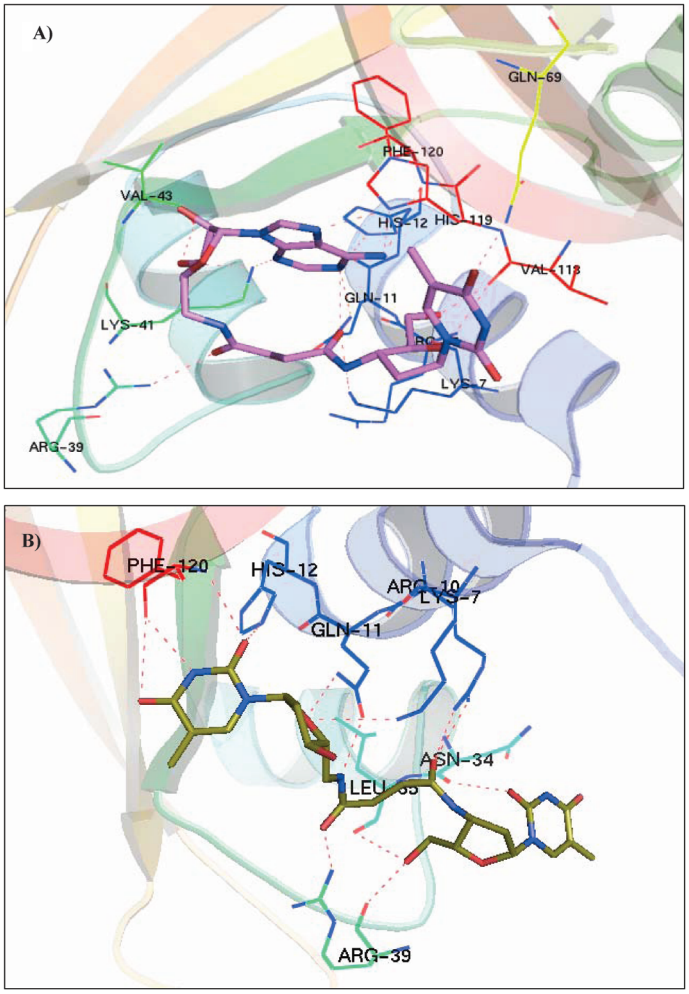

Figure 6. Docked conformation of A) **15** (purple) and B) **11** (yellowish-green) with RNase A (1FS3).

backbone oxygen atom of Val-43 (member of B_1 site) was within a hydrogen-bonding network with the 2′- and 3′-OH groups of the adenine moiety. The amide nitrogen and oxygen atoms (of the linker) are in a position to form a hydrogen-bonding network with Arg-10, Gln-11, and Arg-39 residues. However, for compound **11**, among the three main P_1 site residues, only HIs-12 was found to be within hydrogen-bonding distance (Figure 6B).

Apparently the presence of a carboxylic group (in the linker) for **23** and **21** results in a tighter interaction with the active site residues resulting in favorable ionic interactions with the active site residues. In contrast, there is no such polar ionizable group for **15** and **11**, which have instead a linker that is hydrophobic in nature. This increase in hydrophobicity is manifested by a decrease in inhibition efficacy as reflected from their inhibition constant (K_i) values. Thus **23** and **21** showed better inhibition than **15** and **11**. The successful inhibitory activity of the backbone-modified dinucleosides with polar and nonpolar backbones on RNase A encouraged us to extend this study to angiogenin, the homologue of RNase A that is a potent blood vessel inducer.

Like RNase A the precipitation assay was also conducted in case of angiogenin. The concentration of the five compounds (**23**, **21**, **15**, **11**, and **13**) was fixed at 25 μM with the angiogenin concentration at 0.25 μM. Compounds of this series showed the same trend of ribonucleolytic inhibition of angiogenin as in the case of RNase A (Figure 7). Within the series of compounds, **23** and **21** showed 21 and 17% ribonucleolytic inhibition, respectively, but compound **13** showed only 2% inhibition.

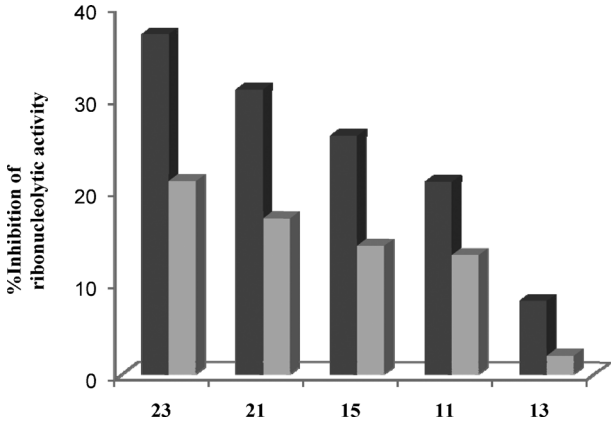

Figure 7. Inhibition of ribonucleolytic activity of RNase A (gray) and angiogenin (black) by backbone modified dinucleosides.

From the precipitation assay it was found that **23** and **21** showed better inhibitory activity compared to the other compounds. Therefore these two compounds were selected for the kinetic study with 6-FAM-dArUdAdA-6-TAMRA as the substrate. The reciprocal of the increase in fluorescence intensity of the fluorescein moiety was plotted against the reciprocal of substrate concentration (Lineweaver–Burk plot), and from the secondary plot we found that the inhibition constant values for **23** and **21** as (670±5) and (729±2) μM, respectively. The nature of the Lineweaver–Burk plots (Figure 8) also indicated the competitive mode of inhibition of the ribonucleolytic activity of angiogenin. The inhibition constant values for compounds **11**, **15**, **21**, and **23** are summarized in Table 1.

Specific protein–ligand interactions for compounds **23** and **21** were also investigated by docking studies. From the docked structure of **23** it was found that the carboxylic group interacted with His-114. On the other hand, three nitrogen atoms of the adenine nucleobase were in a position to form hydrogen bonds with His-13 and Lys-40. The adenine moiety was also found to interact with the B_1 site residue (Leu-115) rather than B_2 site residues. In contrast, the thymine moiety interacted with the B_2 site residue (Gln-108) (Figure 9). The reverse binding observed may be a result of the incorporation of a non-natural backbone between the two nucleosidic moieties. Similarly for **21** (Figure 10) we found the carboxylic group did not interact with any of the His residues of the catalytic site, but was found to be close to Gln-12. Only His-114 was within hydro-

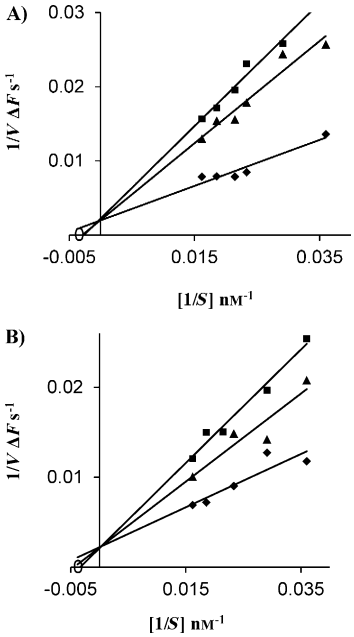

Figure 8. Lineweaver–Burk plots for the inhibition of angiogenin by A) **23**: 0 mM (◆), 0.4 mM (▲) and 1.1 mM (■); B) **21**: 0 mM (◆), 0.6 mM (▲) and 2.3 mM (■). Angiogenin concentration: 0.34 μM.

Table 1. Inhibition constant (K_i) values for compounds **23**, **21**, **15**, and **11**.

	K_i [μM] for RNase A	K_i [μM] for angiogenin
23	(59±3)	(670±5)
21	(155±5)	(729±2)
15	(443±2)	–
11	(544±2)	–

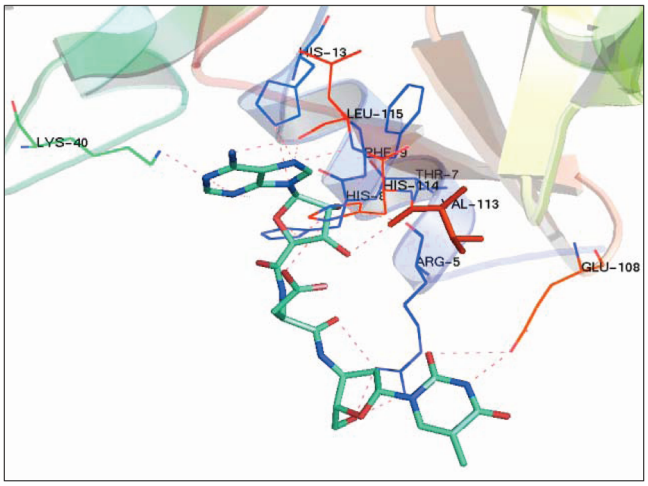

Figure 9. Docked conformation of **23** with angiogenin (1B1I).

gen-bonding distance of a nitrogen atom of the amide bond that serves as the linker.

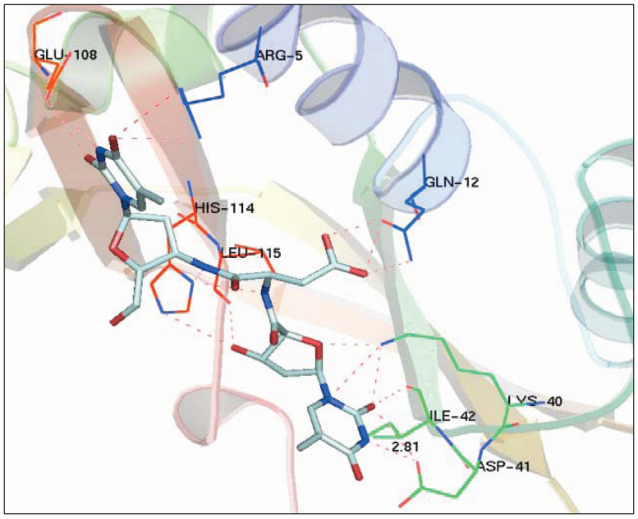

Figure 10. Docked conformation of **21** (cyan) with angiogenin (1B1I).

Conclusion

Backbone-modified non-phosphate-linked dinucleosides have been employed to inhibit the ribonucleolytic activity of RNase A and angiogenin.[35] Among the five members of this series we find that compounds **23** and **21** with a carboxylic group present in the linker region were able to inhibit the ribonucleolytic activity of RNase A and angiogenin more effectively. For both hydrophobic and hydrophilic linkers we find that the thymine–adenine pair was more effective compared to the thymine–thymine pair. Comparing the K_i value of **23** with TpdA-3′-p and TpdA (K_i values are 137 and 1200 μM, respectively),[36,37] we observe that the incorporation of the non-natural backbone in place of phosphate groups effectively enhanced their inhibitory activity towards RNase A. The K_i value of **23** ((59±3) μM) is higher than pTpdA-3′-p (14.2 μM),[36] which is likely due to presence of three highly ionizable phosphate groups. However, for angiogenin the enhancement was more pronounced. The incorporation of this type of non-natural backbone was probably the reason behind their better inhibitory activity. The docking poses of these compounds with RNase A and angiogenin revealed that these compounds interacted typically with the ribonucleolytic site residues. However, it also shows how synthetic modifications of the inhibitors can generate a profound alteration in its mode of interaction with the target protein.

Thus the introduction of a non-natural backbone had been proven to be a good venture for the designing of inhibitors with lower ionic character. We detect that the presence of the non-natural backbone with one carboxylic group was effective in increasing the inhibitory activity of the protein compared to the phosphate analogue. Therefore it is possible that this kind of modification can be utilized for the identification of potent inhibitors of ribonucleases.

Experimental Section

Materials: Bovine pancreatic ribonuclease A (RNase A), recombinant human angiogenin, human serum albumin (HSA), yeast tRNA, 2′,3′-cCMP, D_2O, [D_6]DMSO, $CDCl_3$were from Sigma–Aldrich. 6-FAM-dArU-dAdA-6-TAMRA was purchased from Integrated DNA Technologies (Coralville, IA) and all other reagents (analytical grade) were from SRL (India) and also from Sigma–Aldrich. Column chromatographic separations were performed using silica gel (60–120 and 230–400 mesh). HPLC separations were performed by Shimadru Prominence Series HPLC system. Luna 10 μm C18 column (100 Å) was used for the separation. Solvents were dried and distilled following standard procedures. TLC was carried out on precoated plates (Merck silica gel 60, f_{254}), and the spots visualized with UV light or by charring the plates dipped in 5% H_2SO_4/MeOH solution or 5% H_2SO_4/vanillin/EtOH or 5% ninhydrin in MeOH. ^{1}H NMR (400 MHz) and ^{13}C NMR (100 MHz) spectra were recorded on a Bruker NMR spectrometer (δ scale). UV/Vis measurements were made using a Perkin–Elmer UV/Vis spectrophotometer (Model Lambda 25). Fluorescence measurements were recorded on a Spex Fluorolog-3 machine. Compounds **1**,[38] **5**,[30] **6**,[28] **7**, **8**,[31] and **16**[34] and L-Boc-Asp(OBzl)OH were prepared following literature procedures. Concentrations of the solutions were determined spectrophotometrically using the following data: for RNase A $\varepsilon_{278.5}=9800\,\text{M}^{-1}\,\text{cm}^{-1}$,[39] for 2′,3′-cCMP $\varepsilon_{268}=8500\,\text{M}^{-1}\,\text{cm}^{-1}$,[40] for angiogenin $\varepsilon_{278}=12\,500\,\text{M}^{-1}\,\text{cm}^{-1}$,[41] for 6-FAM-dArUdAdA-6-TAMRA $\varepsilon_{260}=102\,400\,\text{M}^{-1}\,\text{cm}^{-1}$.[41]

Compound 11: A solution of compound **10** (0.2 g, 0.2 mmol) and 50% TFA in CH_2Cl_2 (10 mL) was stirred for 4 h at room temperature. All volatile matters were removed under reduced pressure. The crude residue was purified over silica gel to afford compound **11** (0.1 g, 79%); hygroscopic white solid. ^{1}H NMR: [D_6]DMSO: $\delta=1.78$ (s, 3H), 1.81 (s, 3H), 1.99–2.21 (m, 4H), 2.34 (brs, 4H), 3.27–3.31 (m, 2H), 3.53 (dd, $J=3.6$, 12 Hz, 1H), 3.61 (m, 1H), 3.72 (m, 2H), 4.13, (m, 1H), 4.28 (m, 1H), 6.11–6.20 (m, 2H), 7.50 (s, 1H), 7.77 ppm (s, 1H); ^{13}C NMR [D_6]DMSO: $\delta=12.4$, 12.6, 30.9 (CH_2), 37.3 (CH_2), 38.7 (CH_2), 41.2 (CH_2), 49.4, 61.7 (CH_2), 71.5, 84.0, 84.2, 85.3, 85.4, 109.8 (C), 110.2 (C), 136.6, 150.8 (C), 150.9 (C), 164.2 (C), 172.0 (C), 172.2 ppm (C); HRMS (ESI$^+$): m/z calcd for $C_{24}H_{32}N_6O_{10}Na$ $[M+Na]^+$: 587.2072; found: 587.2054.

Compound 13: A solution of compound **3** (0.4 g, 0.67 mmol) in dry THF (15 mL) was cooled to −15 °C. EDC·HCl (0.18 g, 0. 94 mmol) and HOBT (0.13 g, 0.94 mmol) were added to this solution and the mixture was stirred at 0 °C. After 1 h a solution of compound **5** (0.24 g, 0.67 mmol) in DIEA (0.5 mL, 2.68 mmol), kept at 0 °C, was added to the reaction mixture and the mixture was stirred further for 24 h. After completion of the reaction (TLC), volatile materials were removed under reduced pressure. The residual material was diluted with CH_2Cl_2 and the organic solution was washed with 5% HCl, 10% $NaHCO_3$, and finally with brine. Organic layers were combined, dried over anhyd. Na_2SO_4, filtered and the filtrate was evaporated under reduced pressure. The crude residue was purified over silica gel to afford compound **12** as a gummy solid (41% yield; HRMS (ESI$^+$): m/z calcd for $C_{50}H_{63}N_6O_{10}Si$ $[M+H]^+$: 935.4369; found: 935.4377), which was taken directly for the deprotection step. Thus, a solution of compound **12** (0.16 g, 0.17 mmol) and 50% TFA in CH_2Cl_2 (5 mL) was stirred with for 4 h at room temperature. All volatile matters were removed under reduced pressure. The crude residue was purified over silica gel to afford the compound **13** (0.09 g, 85%); hygroscopic white solid. ^{1}H NMR: [D_6]DMSO: $\delta=1.68$–1.75 (m, 2H), 1.79 (d, $J=$ 8 Hz, 6H), 2.01–2.24 (m, 8H), 3.24 (m, 1H), 3.32–3.35 (m, 1H), 3.54 (dd, $J=3.6$, 12 Hz, 1H), 3.62 (dd, $J=2$, 11.6 Hz, 1H), 3.75 (m, 2H), 4.13 (t, $J=2.8$ Hz, 1H), 4.30 (m, 1H), 6.12–6.20 (m, 2H), 7.48 (s, 1H), 7.78 ppm (s, 1H); ^{13}C NMR [D_6]DMSO: $\delta=12.5$, 12.7, 21.8 (CH_2), 35.0 (CH_2), 37.5 (CH_2), 38.7 (CH_2), 41.3 (CH_2), 49.4, 61.8 (CH_2), 71.6, 84.0, 84.3, 85.4, 85.6, 109.9 (C), 110.2 (C), 136.6, 136.6, 150.8 (C), 150.8 (C), 164.1 (C), 164.2 (C), 172.2 (C), 172.5 ppm (C); HRMS (ESI$^+$): m/z calcd for $C_{25}H_{35}N_6O_{10}$ $[M+H]^+$: 579.2414; found: 579.2406.

Compound 15: A solution of compound **14** (0.24 g, 0.2 mmol) and 50% TFA in CH_2Cl_2 (7 mL) was stirred for 4 h at room temperature. All volatile materials were removed under reduced pressure. The crude residue was purified over silica gel to afford the compound **15** (0.093 g, 71%); hygroscopic white solid. ^{1}H NMR: [D_6]DMSO: $\delta=1.77$ (s, 3H),2.05–2.10 (m, 1H), 2.16–2.21 (m, 1H), 2.36 (m, 3H), 3.28–3.43 (m, 2H), 3.52 (dd, $J=4$, 12 Hz, 1H), 3.60 (m, 1H), 3.74 (m, 1H), 3.95 (m, 1H), 4.02 (m, 1H), 4.29 (m, 1H), 4.67 (t, $J=5.6$ Hz, 1H), 5.83 (d, $J=6$ Hz, 1H), 6.17 (t, $J=6.8$ Hz, 1H), 7.77 (s, 1H), 8.18 (s, 1H), 8.35 ppm (s, 1H); ^{13}C NMR [D_6]DMSO: $\delta=12.6$, 30.9 (CH_2), 37.3 (CH_2), 41.3 (CH_2), 49.3, 61.6 (CH_2), 71.5, 72.9, 83.9, 84.0, 85.4, 88.2, 109.8 (C), 119.8 (C), 136.7, 140.9, 149.5 (C), 150.8 (C), 153.0, 156.5 (C), 164.3, 172.1 (C), 172.2 ppm (C); HRMS (ESI$^+$): m/z calcd for $C_{24}H_{32}N_9O_9$ $[M+H]^+$: 590.2322; found: 590.2315.

Compound 21: 10% Pd/C (0.1 g) was added to a solution of compound **20** (0.09 g, 0.1 mmol) in dry MeOH (10 mL) and the mixture was stirred at 60 °C under H_2 atmosphere. After 8 h (TLC), the mixture was diluted with MeOH and filtered through a bed of Celite, which was further washed several times with MeOH. Combined organic layers were evaporated under reduced pressure. The crude residue was purified with the help of HPLC to afford compound **21** (0.04 g, 68%); hygroscopic white solid.^{1}H NMR: [D_4]MeOH: $\delta=1.88$–1.90 (m, 6H), 2.19 (m, 1H), 2.36 (m, 2H), 2.68 (m, 2H), 3.67–3.89 (m, 4H), 4.36 (brs, 1H), 4.49 (m, 1H), 4.61 (m, 2H), 6.22 (m, 1H), 6.33 (t, $J=6.4$ Hz, 1H), 7.87 (s, 1H), 7.92 ppm (s, 1H); ^{13}C NMR [D_6]DMSO: $\delta=12.0$, 12.1, 35.1 (CH_2), 38.0 (CH_2), 50.2, 52.2, 66.8 (CH_2), 73.7 (CH_2), 77.3, 81.2, 84.4, 84.5, 91.9, 111.2 (C), 111.6 (C), 135.5, 138.9, 150.4 (C), 151.1 (C), 163.6 (C), 163.7 (C), 170.1 (C), 170.2 (C), 175.0 (C); HRMS (ESI$^+$): m/z calcd for $C_{24}H_{30}N_6O_{12}Na$ $[M+Na]^+$: 617.1819; found: 617.1822.

Compound 23: 10% Pd/C (0.1 g) was added to a solution of compound **22** (0.1 g, 0.1 mmol) in dry MeOH (10 mL) and the mixture was stirred at 60 °C under H_2 atmosphere. After 8 h (TLC), the mixture was diluted with MeOH and filtered through a bed of Celite, which was further washed several times with MeOH. Combined organic layers were evaporated under reduced pressure. The crude residue was stirred with 50% TFA in CH_2Cl_2 (3 mL) at room temperature. After 4 h (TLC), all volatile materials were removed under reduced pressure. The crude residue was purified with the help of HPLC to afford compound **23** (0.03 g, 62%); hygroscopic white solid. ^{1}H NMR: [D_4]MeOH: $\delta=1.64$ (s, 3H), 1.80 (dd, $J=5.2$, 16.4 Hz, 1H), 2.20–2.28 (m, 2H), 2.50 (m, 1H), 3.66 (m, 2H), 3.79 (m, 1H), 3.91 (brs, 1H), 4.41 (m, 1H), 4.53–4.62 (m, 2H), 4.83 (d, $J=$ 2 Hz, 1H), 6.22 (d, $J=1.6$ Hz, 1H), 6.32 (t, $J=6$ Hz, 1H), 7.80 (s, 1H), 8.65 (s, 1H), 8.82 ppm (s, 1H); ^{13}C NMR [D_6]DMSO: $\delta=12.0$, 30.9 (CH_2), 37.3 (CH_2), 48.9, 50.9, 66.9, 83.3, 83.4, 84.5, 84.8, 86.9, 91.3, 111.4 (C), 123.8 (C), 136.2, 137.5 (C), 144.4, 149.5 (C), 150.6 (C), 150.9 (C), 152.1, 152.2 (C), 163.9 (C), 173.2 ppm (C). HRMS (ESI$^+$): m/z calcd for $C_{24}H_{29}N_9O_{11}Na$ $[M+Na]^+$: 642.1884; found: 642.1887.

Agarose-gel-based assay: Inhibition of RNase A by all dinucleosides was checked qualitatively by the degradation of tRNA in an agarose gel. In this method, of RNase A (20 μL; 0.66 μM) was mixed with the compounds (10, 15, and 20 μL; 0.92 mM) to a final volume of 50 μL and the resulting solutions were incubated for 6 h at 37 °C. Aliquots (20 μL) from incubated mixtures were then mixed with of tRNA solution (20 μL; 5.0 mg mL^{-1}) and sample buffer (10 μL; containing 10% glycerol and 0.025% bromophenol blue). The mixture was then incubated for another 30 min. A volume of 15 μL from each solution were extracted and loaded onto a 1.1% agarose gel. The gel was run in 0.04 M Tris/acetic acid/EDTA (TAE) buffer (pH 8.0). The undegraded tRNA was visualized by ethidium bromide staining under UV light.

Precipitation assay: Inhibition of the ribonucleolytic activity of RNase A and angiogenin were quantified by the precipitation assay as described by Bond.[42] In this method RNase A (10 μL; 2 μM) was mixed with each dinucleoside (50 μL; 1 mM) to a final volume of 100 μL and incubated for 2 h at 37 °C. An aliquot (20 μL) of the resulting solutions from the incubated mixtures was then mixed with tRNA (40 μL; 5 mg mL^{-1}) and Tris/HCl buffer (40 μL; pH 7.5 containing 5 mM EDTA and 0.5 mg mL^{-1} HSA). After incubation of the reaction mixture at 25 °C for 30 min, of ice-cold perchloric acid (200 μL, 1.14 N; containing 6 mM uranyl acetate) was added to quench the reaction. The solution was then kept in ice for another 30 min and centrifuged at 4 °C at 12000 rpm for 5 min. An aliquot (100 μL) of the supernatant was taken and diluted to 1 mL. The change in absorbance at 260 nm was measured and compared to a control

set. For angiogenin the same method was followed. The concentration of angiogenin and the inhibitors were 0.25 and 25 μM respectively.

Inhibition kinetics: The inhibition of RNase A by **23**, **21**, **15**, **11** was assessed individually by a spectrophotometric method as described by Anderson and co-workers.[40] The assay was performed in oligovinylsulfonic acid free[43] Mes-NaOH buffer (0.1 M, pH 6.0 containing 0.1 M NaCl) using 2′, 3′-cCMP as the substrate. For **23**, **21**, **15**, **11** the inhibitor concentrations were ranged from 0–0.18, 0–0.18, 0–0.39 and 0–0.42 μM, respectively, and the substrate concentrations were used 275–580, 320–650, 220–500 and 350–750 μM, respectively. RNase A concentration was 7.5 μM for all the four compounds. The inhibition constants (K_i) were determined from initial velocity data. The reciprocal of initial velocity was plotted against the inhibitor concentration (Dixon Plot) according to the Equation (1) in which v is the initial velocity, [S] the substrate concentration, [I] the inhibitor concentration, K_m the Michaelis constant, K_i the inhibition constant and V_{max} the maximum velocity.

$$\frac{1}{v} = \frac{K_m}{V_{max}[S]K_i}[I] + \frac{1}{V_{max}}\left[1 + \frac{K_m}{[S]}\right] \quad (1)$$

Purchased recombinant human angiogenin contains a substantial amount of bovine serum albumin (BSA). Pure angiogenin was obtained after removal of BSA using Amicon Ultra centrifugal filter devices (Millipore) with a 30 kD molecular weight cutoff. Purified angiogenin was checked to be free of contaminating ribonucleases by zymogram electrophoresis.[44,45] 6-FAM-dArUdAdA-6-TAMRA was used as a substrate for the kinetic experiment of human angiogenin. Kinetic experiments were carried out in oligovinylsulfonic acid free[43] Mes-NaOH buffer (0.1 M, pH 6.0 containing 0.1 M NaCl), using substrate concentrations from 20 to 122 nM. For **23** and **21**, the concentration ranged from 0 to 1.1 and 0 to 2.3 mM, respectively. The angiogenin concentration was 0.23 μM. An increase in fluorescence emission intensity at 515 nm, upon excitation at 490 nm, indicates the progress of the reaction.[46] The inhibition constants (K_i) were determined from initial velocity data using Lineweaver–Burk plots—Equation (2), in which v is the initial velocity, [S] the substrate concentration, [I] the inhibitor concentration, K_m the Michaelis constant, K_i the inhibition constant and V_{max} the maximum velocity.

$$\frac{1}{v} = \frac{K_m}{V_{max}}\left(1 + \frac{[I]}{K_i}\right)\frac{1}{[S]} + \frac{1}{V_{max}}\left(1 + \frac{[I]}{K_i}\right) \quad (2)$$

Docking studies: The crystal structure of RNase A and human angiogenin (PDB entry 1FS3 and 1B1I, respectively) was downloaded from the Protein Data Bank.[47] The 3D structures of the backbone modified dinucleosides were generated by Sybyl6.92 (Tripos Inc., St. Louis, USA) and their energy-minimized conformations were obtained with the help of the MMFF96 force field using MMFF96 charges with a gradient of 0.005 kcal mol^{-1}. The FlexX software as part of the Sybyl suite was used for docking of the dinucleosides with RNase A. PyMol[48] was used for visualization of the docked conformations.

Acknowledgements

J.D. thanks CSIR, India for a fellowship. S.D. and T.P. are grateful to the Department of Science and Technology (DST), New Delhi, India, for financial support. J.D. thanks Dr. Kalyan S. Ghosh for his unforgettable help in HPLC purification.

[1] J. W. Fett, D. J. Strydom, R. R. . Lobb, E. M. Alderman, J. L. Bethune, J. F. Riordan, B. L. Vallee, *Biochemistry* **1985**, *24*, 5480–5486.
[2] D. J. Strydom, *Cell. Mol. Life Sci.* **1998**, *54*, 811–824.
[3] J. Badet, F. Soncin, J. D. Guitton, O. Lamare, T. Cartwright, D. Barritault, *Proc. Natl. Acad. Sci. USA* **1989**, *86*, 8427–8431.
[4] R. Bicknell, B. L. Vallee, *Proc. Natl. Acad. Sci. USA* **1988**, *85*, 5961–5965.
[5] F. Soncin, *Proc. Natl. Acad. Sci. USA* **1992**, *89*, 2232–2236.
[6] G. F. Hu, J. F. Riordan, *Biochem. Biophys. Res. Commun.* **1993**, *197*, 682–687.
[7] G. F. Hu, J. F. Riordan, b. L. Vallee, *Proc. Natl. Acad. Sci. USA* **1994**, *91*, 12096–12100.
[8] S. I. Jimi, K. I. Ito, K. Kohno, M. Ono, M. Kuwano, Y. Itagaki, H. Isikawa, *Biochem. Biophys. Res. Commun.* **1995**, *211*, 476–483.
[9] J. Folkman, M. Klagsbrun, *Science* **1987**, *235*, 442–447.
[10] P. A. Leland, K. E. Staniszewski, C. Park, B. R. Kelemen, R. T. Raines, *Biochemistry* **2002**, *41*, 1343–1350.
[11] a) G. J. Gleich, D. A. Loegering, M. P. Bell, J. L. Checkel, S. J. Ackerman, D. J. McKean, *Proc. Natl. Acad. Sci. USA* **1986**, *83*, 3146–3150; b) D. D. Leonidas, E. Boix, R. Prill, M. Suzuki, R. Turton, K. Minson, G. J. Swaminathan, R. J. Youle, K. R. Acharya, *J. Biol. Chem.* **2001**, *276*, 15009–15017.
[12] C. G. Mohan, E. Boix, H. R. Evans, Z. Nikolovski, M. V. Nogue's, C. M. Cuchillo, K. Ravi Acharya, *Biochemistry* **2002**, *41*, 12100–12106.
[13] B. M. Fisher, J. E. Grilley, R. T. Raines, *J. Biol. Chem.* **1998**, *273*, 34134–34138.
[14] R. Shapiro, J. F. Riordan, B. L. Vallee, *Biochemistry* **1986**, *25*, 3527–3532.
[15] R. Shapiro, S. Weremowicz, J. F. Riordan, B. L. Vallee, *Proc. Natl. Acad. Sci. USA* **1987**, *84*, 8783–8787.
[16] R. Shapiro, B. L. Vallee, *Biochemistry* **1989**, *28*, 7401–7408.
[17] T. P. Curran, R. Shapiro, J. F. Riordan, *Biochemistry* **1993**, *32*, 2307–2313.
[18] A. Russo, K. R. Acharya, R. Shapiro, *Methods Enzymol.* **2001**, *341*, 629–648.
[19] K. Kumar, J. L. Jenkins, A. M. Jardine, R. Shapiro, *Biochem. Biophys. Res. Commun.* **2003**, *300*, 81–86.
[20] G. I. Yakovlev, V. A. Mitkevich, A. A. Makarov, *Mol. Biol.* **2006**, *40*, 867.
[21] A. G. McLennan, *Pharmacol. Ther.* **2000**, *87*, 73–89.
[22] D. D. Leonidas, R. Shapiro, L. I. Irons, N. Russo, K. R. Acharya, *Biochemistry* **1999**, *38*, 10287–10297.
[23] A. M. Jardine, D. D. Leonidas, J. L. Jenkins, C. Park, R. T. Rains, K. R. Acharya, R. Shapiro, *Biochemistry* **2001**, *40*, 10262–10272.
[24] K. Tonan, P. Xu, J. L. Jenkins, A. Russo, R. Shapiro, F. Ni, *Biochemistry* **2003**, *42*, 11137–11149.
[25] J. Debnath, S. Dasgupta, T. Pathak, *Bioorg. Med. Chem.* **2009**, *17*, 4921–4927.
[26] J. Debnath, S. Dasgupta, T. Pathak, *Bioorg. Med. Chem.* **2009**, *17*, 6491–6495.
[27] A. Samanta, D. D. Leonidas, S. Dasgupta, T. Pathak, S. E. Zographos, N. G. Oikonomakos, *J. Med. Chem.* **2009**, *52*, 932–942.
[28] G. H. Jones, M. Taniguchi, D. Tegg, J. G. Moffatt, *J. Org. Chem.* **1979**, *44*, 1309–1317.
[29] R. S. Varma, M. E. Hogan, *Tetrahedron Lett.* **1992**, *33*, 7719–7720.
[30] I. Kers, J. Stawinski, A. Kraszewski, *Tetrahedron* **1999**, *55*, 11579–11588.
[31] H. Ikeuchi, M. E. Meyer, Y. Ding, J. Hiratake, N. G. J. Richards, *Bioorg. Med. Chem.* **2009**, *17*, 6641–6650.
[32] M. Albrecht, M. Napp, M. Schneider, *Synthesis* **2001**, 0468–0472.
[33] a) M. Bartra, P. Romea, F. Urpí, J. Vilarrrasa, *Tetrahedron* **1990**, *46*, 587–594; b) R. C. Claussen, B. M. Rabatic, S. I. Stupp, *J. Am. Chem. Soc.* **2003**, *125*, 12680–12681.
[34] H. B. Lazrek, J. W. Engels, W. Pfleiderer, *Nucleoside Nucleotide* **1998**, *17*, 1851–1856.
[35] There is only one report so far on the use of backbone-modified non-phosphate linked dinucleosides as RNase A inhibitors, see: N. Thiyagarajan, B. D. Smith, R. T. Raines, K. R. Acharya, *FEBS J.* **2011**, *278*, 541–549.
[36] M. Irie, H. Watanabe, K. Ohgi, M. Tobe, G. Matsumura, Y. Arata, T. Hirose, S. Inayama, *J. Biochem.* **1984**, *95*, 751–759.
[37] N. Russo, R. Shapiro, *J. Biol. Chem.* **1999**, *274*, 14902–14908.
[38] J. Debnath, S. Dasgupta, T. Pathak, *Bioorg. Med. Chem.* **2010**, *18*, 8257–8263.
[39] M. Sela, C. B. Anfinsen, *Biochim. Biophys. Acta.* **1957**, *24*, 229–235.

[40] D. G. Anderson, G. G. Hammes, F. G. Walz, *Biochemistry* **1968**, *7*, 1637–1645.
[41] R. T. Raines, M. P. Toscano, D. M. Nierengarten, J. H. Ha, R. Auerbach, *J. Biol. Chem.* **1995**, *270*, 17180–17184.
[42] M. D. Bond, *Anal. Biochem.* **1988**, *173*, 166–173.
[43] B. D. Smith, M. B. Soellner, R. T. Raines, *J. Biol. Chem.* **2003**, *278*, 20934–20938.
[44] A. Blank, R. H. Sugiyama, C. A. Dekker, *Anal. Biochem.* **1982**, *120*, 267–275.
[45] J.-S. Kim, R. T. Raines, *Protein Sci.* **1993**, *2*, 348–356.
[46] B. R. Kelemen, T. A. Klink, M. A. Behlke, S. R. Eubanks, P. A. Leland, R. T. Raines, *Nucleic Acids Res.* **1999**, *27*, 3696–3701.
[47] H. M. Berman, J. Westbrook, Z. Feng, G. Gilliland, T. N. Bhat, H. Weissig, I. N. Shindyalov, P. E. Bourne, *Nucleic Acids Res.* **2000**, *28*, 235–242.
[48] W. L. DeLano, The PyMOL Molecular Graphics System, DeLano Scientific, San Carlos, CA, 2004. USA. http://pymol.sourceforge.net/.

Received: September 8, 2011
Published online: January 19, 2012

